Journal of Energy Storage 44 (2021) 103441

Contents lists available at ScienceDirect

Journal of Energy Storage

journal homepage: www.elsevier.com/locate/est

Advanced parametrisation of phase change materials through kinetic approach

Jesus Lizana [a,b,*], Antonio Perejón [c,*], Pedro E. Sanchez-Jimenez [a,c], Luis A. Perez-Maqueda [a,*]

[a] Instituto de Ciencia de Materiales de Sevilla, Consejo Superior de Investigaciones Científicas, Universidad de Sevilla, Calle Américo, Vespucio 49, 41092 Seville, Spain
[b] Department of Engineering Science, University of Oxford, Parks Road, Oxford OX1 3PJ, United Kingdom
[c] Departamento de Química Inorgánica, Facultad de Química, Universidad de Sevilla, Calle Profesor García González 1, 41012 Seville, Spain

ARTICLE INFO

Keywords:
Phase change material
Heat transfer
Latent heat
Kinetic
Subcooling
Thermal energy storage

ABSTRACT

Phase change materials (PCM) have been widely investigated for heat storage and transfer applications. Numerous numerical simulation approaches have been proposed for modelling their behaviour and predicting their performance in thermal applications. However, simulation approaches do not consider the kinetics of the phase transition processes, compromising the accuracy of their predictions. The phase change is a kinetically driven process in which both the reaction rate and the reaction progress depend on the heating schedule. This work evaluates and parametrises the influence of kinetics in the melting and crystallisation behaviour of a well-known PCM, PEG1500, and compares potential discrepancies with common phase change parametrisation alternatives. The kinetic dependence was experimentally evaluated through differential scanning calorimetry (DSC). The kinetic parameters required for modelling the kinetics of the processes were determined by both model-free and model-fitting procedures following ICTAC (International Confederation for Thermal Analysis and Calorimetry) recommendations. Then, the phase transition was parametrised through a kinetic model and compared with three conventional phase transition models: linear without hysteresis, non-linear without hysteresis, and non-linear with hysteresis. The statistical comparison between models demonstrates the higher accuracy of the kinetic approach to correctly represent the partial enthalpy distribution of latent heat storage materials during alternative phase change rates, obtaining a coefficient of determination (R^2) of 0.80. On the other hand, the accuracy of kinetic-independent models is limited to the range from 0.40 to 0.61. The results highlight the high discrepancies of conventional models compared to the kinetic approach and provide criteria and guidelines for efficient kinetic modelling of phase change in heat transfer evaluations.

1. Introduction

Phase change materials (PCMs) have attracted considerable attention for thermal energy storage (TES) applications [1,2] as they show benefits related to their high TES density [3], constant temperature [4] and reduced heat losses [5]. The thermophysical properties of PCMs have been widely investigated in the literature in order to achieve an adequate phase change temperature for the corresponding TES application, high latent and specific heat capacity, high thermal conductivity and good thermal stability and reliability under cycling [6]. An extensive portfolio of commercial PCMs is available in the market [7]. Furthermore, numerous mathematical and numerical simulation approaches of PCMs have been proposed to evaluate potential applied energy solutions with a considerable saving in time and investment in techno-economic evaluations [8–10]. However, all the numerical modelling approaches are based on kinetic-independent phase transition functions defined through experimental or commercial data, whose performance could not represent the final PCM behaviour.

There are different approaches to characterise and parametrise the phase change in heat transfer energy models. Most used parametrisation approaches are based on the definition of phase change through linear transition functions, non-linear functions, linear or non-linear functions with hysteresis, or the direct use of experimental data.

Linear transition functions represent the most extended parametrisation approach to define phase change fraction as a function of the temperature [11]. This two-phase linear model is usually determined through tabulated data from differential scanning calorimetry (DSC) measurements or simple commercial information (i.e. total latent heat capacity, kJ/kg) in order to define enthalpy-temperature or apparent

* Corresponding authors.
E-mail addresses: lizana@icmse.csic.es (J. Lizana), antonio.perejon@icmse.csic.es (A. Perejón), maqueda@icmse.csic.es (L.A. Perez-Maqueda).

https://doi.org/10.1016/j.est.2021.103441
Received 4 August 2021; Received in revised form 7 October 2021; Accepted 11 October 2021
Available online 2 November 2021

Nomenclature

A	Arrhenius preexponential factor, s^{-1}
c_p	specific heat, $J{\cdot}g^{-1}{\cdot}K^{-1}$
$\widetilde{c}_p$	apparent specific heat, $J{\cdot}g^{-1}{\cdot}K^{-1}$
DSC	differential scanning calorimetry
Ea	activation energy, $J{\cdot}mol^{-1}$
h	hill slope
ICTAC	International Confederation for Thermal Analysis and Calorimetry
In	indio
m_i	measured value
n	number of measured data points
PCM	phase change material
PEG	Poly(ethylene glycol)
R	universal gas constant, 8.3145 $J{\cdot}K^{-1}{\cdot}mol^{-1}$
R^2	coefficient of determination
s	control factor
s_i	Simulated value
t	time
T	temperature, °C
TES	thermal energy storage

Greek letters

α	solid-liquid conversion, being 0 is fully solid state and 1 for a fully liquid state.
ΔH	latent heat capacity, $J{\cdot}g^{-1}$

Subscript and superscript

l	liquid
max	maximum
min	minimum
s	solid

heat capacity-temperature curves in a simple way. For example, Ascione et al. [12] used this approach to characterise the enthalpy-temperature curve to evaluate the benefits of PCM plaster to improve building performance. Diaconu and Cruceru [13] simulated with this approach the performance of a PCM wall. Lizana et al. [14] defined a linear enthalpy-temperature curve to simulate the performance of a latent heat storage tank in TRNSYS software. Xu et al. [15] considered a linear liquid fraction for evaluation of the interface evolution of a PCM with/without porous media, and Xu and Zhao [16] for the thermal efficiency analysis of cascaded latent heat/cold storage.

Another widely used approach is based on the definition of transition curves through non-linear functions, such as probability distribution functions [17,18] or cubic spline interpolating polynomials [19], whose parametrisation corresponds to the fitting of phase transition model to experimental data by numerical solution of a non-linear regression problem. For example, Piselli et al. [20] defined non-linear enthalpy--temperature function for PCM board using commercial data, and Biswas et al. [21] modelled enthalpy curve through a Gaussian function.

Other simulation approaches implement two hystereses through linear or non-linear functions to consider the material's subcooling effect. For example, Hu and Heiselberg [22] evaluated the performance of a new ventilated window with a PCM heat exchanger considering PCM hysteresis in COMSOL Multiphysics. However, this hysteresis model is not often considered in the modelling of PCM systems [9], and according to Moreles et al. [23], it can have a significant influence on the final performance. Additionally, other numerical methods can implement experimental heat capacity-temperature data obtained from DSC measurements to define two separate enthalpy curves for melting and freezing in order to consider the hysteresis effect. This approach was used by Lizana et al. [24] to simulate PCM-based passive cooling applications' performance. All these phase transition parametrisation alternatives have been widely used in the enthalpy-based method, apparent heat capacity method and heat source method, among others, to simulate PCM-based applications [25,26]. A detailed definition of these numerical simulation methods is provided by Asgharian and Baniasadi [8].

It should be highlighted that all these previous parametrisation approaches are based on static phase transition models, which are independent of the heating or cooling rate. The kinetics of the phase transition processes has been seldom considered in PCM numerical modelling [8,27]. The kinetics of phase change refers to modifying melting or solidification conditions based on the reaction rate and the reaction progress. While for the static hysteresis model, the phase change is modelled with two static curves, one for melting and another for solidification, in the kinetic model, the phase change is defined as an intrinsic dynamic variable as a function of temperature (T) and time (t). Thus, in this case, melting and crystallisation behaviour (or curve) will depend on rate function k(T) and reaction function f(α) that characterise the kinetic model.

Heating and cooling rates can widely influence PCM performance, as heat capacity and crystallisation temperatures are highly affected by operating conditions. In this case, a kinetic model, commonly applied in solid-state reactions [28–33], can be used to define through a mathematical description the course of the reaction for each step as a function of conditions in the system [34]. This parametrisation model can support the macroscopic modelling approach of PCM regions in which phase change occurs over a temperature range, in which solid and liquid phases coexist. For example, Paberit et al. [27] evaluated the phase transition for different thermal conditions of Poly(ethylene glycol) (PEG) of six molecular weights, showing how the degree of supercooling is dependent on the cooling rate. The results demonstrate that the characterisation of PEGs and their composites should be conducted by parametrising kinetic performance. Moreover, it should be noted that although characterisation of phase transition at heating and cooling rates close to the thermal conditions of the intended TES application can be carried out, a modification of operating conditions will not reflect the appropriate material performance. The kinetics of phase change is an essential issue to be considered [35] since it can largely affect the heat transfer capacity of the PCM region [36,37].

This work evaluates the kinetic influence in PCM's melting and crystallisation behaviour and compares the potential discrepancies between the parametrisation alternatives of phase transition in PCM numerical modelling. Polyethylene glycol (PEG) with an average molar mass of 1500 was selected as reference material. The kinetic dependence of phase transition was experimentally evaluated through differential scanning calorimetry (DSC), and the kinetic parameters (activation energy, preexponential factor and kinetic model) were determined by both model-free and model-fitting approaches following the recommendation of the International Confederation for Thermal Analysis and Calorimetry (ICTAC) [29,38]. Then, the phase transition was parametrised through a kinetic model and compared with three conventional phase transition models: linear without hysteresis, non-linear without hysteresis, and non-linear with hysteresis. Finally, the phase transition parametrisations were compared at different heating and cooling induced rates from the point of view of phase conversion and partial enthalpy-temperature evolution, highlighting discrepancies in material performance and providing criteria for efficient PCM numerical modelling. The main research contributions in this work are:

- Experimental kinetic characterisation of PEG1500, highlighting the high kinetic-dependent phase transition of material and determining the kinetic parameters that describe the phase transition process.
- Systematic definition and application of different parametrisation alternatives for phase change modelling, using PEG 1500 as a reference material. Measured and numerical models are compared and discussed. It involves the first kinetic model of PEG1500, whose kinetic parameters were obtained through model-free (isoconversional) and model-fitting (combined kinetic analysis) approaches.
- Identification of discrepancies in material performance through kinetic-independent and kinetic-dependent phase transition models, providing criteria and guidelines for a reliable PCM characterisation and modelling.

The paper is structured as follows. First, the PCM material, experimental characterisation methods and parametrisation alternatives of phase change are described. Afterwards, the results and discussion are provided, which are divided into four sections: thermal and kinetic characterisation of PEG1500, parametrisation results of phase transition models, evaluation of phase transition models through temperature-induced, and statistical comparison of partial enthalpy distribution obtained per phase transition model for energy balance problems. Finally, the conclusions are provided, highlighting discrepancies between PCM modelling alternatives and providing guidelines for reliable numerical modelling of PCM.

2. Materials and methods

2.1. Materials

PEG1500 was commercially provided by Sigma-Aldrich, whose properties are detailed in Table 1.

This PCM has been widely studied due to their favourable properties for thermal energy storage applications. PEG1500 has an adequate melting temperature for low-to-moderate heat storage and high latent heat capacity with chemical and thermal stability under cycling [39]. Moreover, it is non-flammable, non–toxic, non–corrosive and has a low-to-moderate cost [6]. As a disadvantage, it presents low thermal conductivity as other organic materials.

2.2. Experimental characterisation methods

Latent heat capacity, melting temperature and kinetic performance of PCM at different heating/cooling rates were evaluated using Differential scanning calorimetry (DSC). DSC Q200 instrument from TA Instruments company was used, which measures the difference in the heat flow rate between a sample and inert reference as a function of time and temperature. The apparatus was calibrated using the melting temperature and latent heat of a standard certified reference material (In). DSC samples were encapsulated in hermetic aluminium pans with a mass between 5.00 and 10.00 mg. This thermal analysis using low mass improves heat transfer and minimises thermal gradients within the sample, as is recommended by ICTAC [29,38]. Tzero Pans (container of the sample material) and Tzero hermetic Lids (cap of the container) were used. The first cycle was omitted as it reflects the previous thermal history of the material. Moreover, this first premeeting ensures good contact between the sample and the crucible, necessary for reliable results. Measurements were carried out in a temperature range from 0 to 75 °C with heating/cooling rates of 0.5, 1, 2.5, 5, 10 and 20 °C·min^{-1}, under a purified nitrogen atmosphere with a flow rate of 50 ml·min^{-1}. The melting onset temperatures were obtained by the tangent at the point of the largest slope on the DSC curve. The latent heats of phase change were determined by numerical integration of the area under the peaks.

Specific heat capacity (c_p) was measured with a Sensys Evo (DSC) instrument from SETARAM Instrumentation using a continuous c_p determination programme. This instrument is a CALVET calorimeter with 3D sensor, that totally surrounds the sample so that the entire energy of any transformation is monitored. The instrument was calibrated using the Joule effect. A mass of 97.7 mg was employed in an aluminium crucible, and the first cycle was also omitted. Measurement was carried out in a temperature range from -20 to 80 °C with a heating rate of 2 °C·min^{-1}, under a purified nitrogen atmosphere with a flow rate of 30 ml·min^{-1}.

Table 1
Physical properties of PEG1500 (data provided by Sigma-Aldrich).

Property	Units	Value
Density (20 °C)	Kg·m^{-3}	1200
Melting temperature	°C	43–59
Average molecular mass	g·mol^{-1}	1400–1600
CAS number		25322–68–3

2.3. Structure and parametrisation of phase change modelling approaches

The parametrisation of phase change is carried out through three conventional models (or kinetic-independent phase transition models) and one kinetic model (kinetic-dependent model). They simulate the overall structure of PCM by one characteristic parameter, alpha (α), which range from 0 to 1 in order to simulate the solid-liquid conversion (or phase change) from a fully solid state (α=0) to a fully liquid state (α=1).

Kinetic-independent phase transition models are a static linear model (linear without hysteresis), a static non-linear model (non-linear without hysteresis) and a static hysteresis model (non-linear with hysteresis). The kinetic-dependent phase transition model (kinetic model) is based on a kinetic parametrisation for α. Further details of the structure and parametrisation approaches for each model are defined below.

2.3.1. Static linear model through linear regression

The simplest approach for modelling phase change consists of a static linear transition, which models solid-liquid conversion from 0 (fully solid) to 1 (fully liquid) using a linear regression according to Eq. (1). Experimental data obtained at a heating rate of 5 °C·min^{-1} were used for this modelling approach.

$$\alpha = \alpha(T) = a + b \cdot T \tag{1}$$

2.3.2. Static non-linear model through logistic regression

A more detailed static non-linear model is defined through a sigmoidal function. In this case, a five parameters logistic regression is used to determine the solid-liquid conversion from 0 to 1, according to Eq. (2). The experimental curve obtained at a heating rate of 5 °C·min^{-1} was used for this modelling approach.

$$\alpha = \alpha(T) = \alpha_{min} + \frac{\alpha_{max}\alpha_{-min}}{\left(1 + \left(\frac{T_0}{T}\right)^h\right)^s} = 0 + \frac{1}{\left(1 + \left(\frac{T_0}{T}\right)^h\right)^s} \tag{2}$$

where:

T_0: temperature of half conversion;
h: hill slope;
s: control factor

2.3.3. Static hysteresis model

Static hysteresis is an extension of the static non-linear model, which considers the subcooling behaviour of the material. In this case, the phase change is modelled with two static curves, one for melting and another for solidification. These static curves are independent of the heating or cooling schedule followed by the material. Thus, PEG1500 is modelled following two sigmoidal functions, one five parameters lo-

gistic regression identical to previous Eq. (2) for the heating process, and another one fitting the cooling/solidification process. The sign of the temperature rate (dT/dt) is used to distinguish between heating and cooling curves according to Eq. (3). Experimental heating and cooling curves obtained at 5 °C•min^{-1} were used for this modelling approach.

$$\alpha = \alpha\left(\mathrm{T}, \mathrm{sign}\frac{dT}{dt}\right) \tag{3}$$

2.3.4. Kinetic model

The kinetic model considers a kinetic-dependent phase transition for α. It requires the definition of solid-liquid transition, from 0 to 1, as an intrinsic dynamic variable as a function of temperature (T) and time (t). The kinetic-dependent transition of this thermally stimulated process is parameterised in terms of T and α according to Eq. (4) [34], which describes solid-state processes far from equilibrium by multiplying two functions related with the dependence on temperature (or rate function) $k(T)$ and the reaction function $f(\alpha)$:

$$\frac{d\alpha}{dt} = k(T) \cdot f(\alpha) \tag{4}$$

where:

t: time,

T: temperature,

α: phase change conversion from 0 to 1.

The rate function, $k(T)$, is almost universally represented by the Arrhenius equation (Eq. (5)).

$$k(T) = Ae^{-Ea/RT} \tag{5}$$

where:

A: Arrhenius preexponential factor

Ea: activation energy

R: universal gas constant

The kinetic analysis is divided into two steps. Firstly, model-free (isoconversional) kinetic analysis was used to determine the activation energy (Ea) and evaluate if the kinetic process can be considered a simple process with constant activation energy. Secondly, the combined kinetic analysis was used to validate the results obtained through the isoconversional method and calculate the global kinetic parametrisation associated with the solid-liquid transition. Kinetic analysis was performed following the ICTAC kinetics committee recommendations for performing kinetic computations [29]. Further details are described below:

Model-free (Isoconversional) kinetic analysis. The Friedman isoconversional method [40] was used to estimate the activation energy of the solid-liquid transition as a function of the extent of conversion. This method provides the activation energy without considering the kinetic model followed by the process, and it is based on Eq. (6), obtained from Eqs. (4) and (5) [41].

$$ln\left(\frac{d\alpha}{dt}\right)_{\alpha} = C - \frac{Ea_{\alpha}}{RT_{\alpha}} \tag{6}$$

Where C = ln(Af(α)) is constant for a constant value of the extent of conversion. Thus, the activation energy values for given values of α are obtained from the slope of the plot of $ln\left(\frac{d\alpha}{dt}\right)_{\alpha}$ versus $\frac{1}{T_{\alpha}}$.

Model-fitting (combined kinetic analysis). The combined kinetic analysis [28] was developed to determine the kinetic triplet (E, A and $f(\alpha)$) associated to the solid-liquid transition, without assuming a kinetic model for the process. Thus, the reaction function, $f(\alpha)$, is defined following the general form shown in Eq. (7) (modified Sestak-Berggren equation), which can accurately fit every ideal kinetic model proposed in the literature by adjusting the parameters n and m [28,42].

$$f(\alpha) = c(1-\alpha)^n\ \alpha^m \tag{7}$$

This equation simplifies the kinetic analysis since the kinetic model is determined in a second step with the help of master plots.

The kinetic equation for the combined kinetic analysis is obtained from the general kinetic equation (considering Eqs. (4), (5) and (7)), by taking logarithms and reorganising the terms (Eq. (8)):

$$ln\left(\frac{\frac{d\alpha}{dt}}{(1-\alpha)^n\ \alpha^m}\right) = \ln(cA) - \frac{Ea}{RT} \tag{8}$$

A set of different curves measured under different temperature programs is substituted into the equation, and the left-hand side is plotted versus 1/T. An optimisation procedure is employed for calculating the parameters n and m that give the best linear fit to the plot, and the values of Ea and ln(cA) are obtained from the slope and intercept, respectively.

2.4. Simulation of phase transition models

The parametrised phase transition models, defined in Section 2.3, were implemented into a numerical simulation algorithm developed in Python code. This numerical modelling calculates the conversion progress through constant and variable temperature programmes. However, it should also be noted that certain assumptions need to be made for the hysteresis modelling, particularly when the process is reversed while the material is still within the phase change range [17]. Thus, in the case of hysteretic transition behaviour, related to a change of direction (or hysteresis) in the middle of conversion progress, the mathematical model proposed by Ivshin and Pence [43], defined in Eq. (9), is used to simulate the transition hysteresis. This transition modelling is considered in the static hysteresis model (depicted in Section 2.3.3).

$$\begin{aligned}
\alpha(t_i) &= 1 - \frac{1-(\mathrm{t}_{i-1})}{1-_{heat}(T(\mathrm{t}_{i-1}))} \cdot (1 - \alpha_{hrat} - (T(t_i)))\ if\ sign\frac{dT}{dt} \geq 0 \\
\alpha(t_i) &= \frac{\alpha(t_{i-1})}{\alpha_{cool}(T(t_{i-1}))} \cdot \alpha_{cool}(T(t_i))\ if\ sign\frac{dT}{dt} \leq 0
\end{aligned} \tag{9}$$

where:

$\alpha(\mathrm{t}_{i-1})$: initial conversion situation (t_{i-1})

$\alpha_{heat}(T(\mathrm{t}_{i-1}))$: expected situation for the initial conversion (t_{i-1}) in heating hysteresis

$\alpha_{heat}(T(\mathrm{t}_i))$: expected situation for the conversion at time (t_i) in heating hysteresis

$\alpha_{cool}(T(\mathrm{t}_{i-1}))$: expected situation for the initial conversion (t_{i-1}) in cooling hysteresis

$\alpha_{cool}(T(\mathrm{t}_i))$: expected situation for the conversion at time (t_i) in cooling hysteresis

The capabilities of the numerical modelling approaches were tested using two temperature test profiles, T(t). The first temperature programme consists of sequential heating and cooling ramps of 10, 5, 2.5, 1 and 0.5 °C·min^{-1} from 10 to 70 °C. The second temperature programme is based on three heating and cooling ramps of 1, 2.5 and 5 °C·min^{-1}, in which temperature direction is sequentially changed in the middle of the conversion progress.

2.5. Determination of apparent heat capacity for heat transfer in energy balance models

The apparent specific heat capacity (or partial enthalpy distribution) is obtained for each phase transition model according to Eq. (10) [17, 44], which combines the sensible and latent heat terms into a single linear formulation [45].

$$\widetilde{c}_p = (1-\alpha)c_p^s + \frac{d\alpha}{dT}\Delta H + \alpha \cdot c_p^l \tag{10}$$

where:

c_p^l: specific heat capacity in liquid phase, $J{\cdot}g^{-1}{\cdot}K^{-1}$
c_p^s: specific heat capacity in solid phase, $J{\cdot}g^{-1}{\cdot}K^{-1}$
α: phase change conversion, from 0 to 1
ΔH : latent heat capacity, $J{\cdot}g^{-1}$
With this modelling approach, having α and T is possible to calculate the apparent heat capacity of the material.

2.6. Statistical comparison of phase transition models

The accuracy of phase transition models was statistically evaluated and compared using the coefficient of determination (R^2 or R-squared), a statistical index commonly used to measure how close simulated values are to the regression line of the measured values [46,47]. It is expressed in Eq. (11), where m_i is the measured value, s_i is the simulated one and n the number of measured data points. The result ranges between 0.00 and 1.00, where the higher the value of R^2, the more successful the simulated values match the measured ones.

$$R^2 = \left(\frac{n \cdot \sum_{i=1}^{n} m_i \cdot s_i - \sum_{i=1}^{n} m_i \cdot \sum_{i=1}^{n} s_i}{\sqrt{\left(n \cdot \sum_{i=1}^{n} m_i^2 - \left(\sum_{i=1}^{n} m_i \right)^2 \right) \cdot \left(n \cdot \sum_{i=1}^{n} s_i^2 - \left(\sum_{i=1}^{n} s_i \right)^2 \right)}} \right)^2 \quad (11)$$

3. Results and discussion

The results are shown and discussed in four sections related to the thermal and kinetic characterisation of PEG1500, parametrisation results of phase transition models, evaluation of phase transition models through temperature-induced, and statistical comparison of phase transition models for heat transfer in energy balance models.

3.1. Thermal and kinetic characterisation of PEG1500

The experimental DSC curves registered under different heating and cooling rates are illustrated in Fig. 1. The first cycle was omitted as it reflects the previous thermal history of the material. Fig. 2a shows the normalised DSC signals of melting and crystallisation, and Fig. 2b the cumulative normalised phase transition, from 0 (fully solid) to 1 (fully liquid), as determined from experimental DSC curves in Fig. 1.

The results show a non-ideal phase transition behaviour, where solid-liquid conversion takes place over a temperature range in which both phases coexist. All heating curves have the same melting point at 37.0 °C, and a latent heat capacity of 158.8 $J{\cdot}g^{-1}$ (±2).

The DSC curves show that PEG1500 melting is a thermodynamically-controlled process. The broadening of the experimental curves as the heating rate increases is mainly due to different phenomena associated with heat conduction in the pans, heat transfer and apparatus design [17]. This is also justified since all heating curves have the same onset temperature at approximately 32.5 °C and melting point at 37.0 °C. Conversely, the crystallisation temperature of PEG1500 is highly affected by the cooling rate, showing different subcooling grades in their hysteresis under different cooling rates. Thus, the crystallisation point is reduced as the cooling rate increases. These results demonstrate the significant influence of kinetics on the crystallisation process.

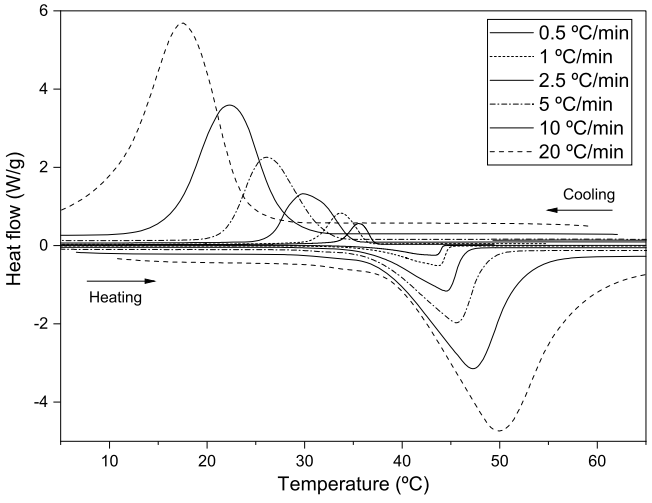

Fig. 1. DSC curves of PEG1500 for heating (melting) and cooling (solidification) at different temperature rates.

This supercooling effect is found in many PCMs for thermal energy storage applications, such as salt hydrates and sugar alcohols [7,48,49]. And it is strongly affected by the cooling or heating rate, as we can see in Figs. 1 and 2. The higher rate, the more considerable subcooling hysteresis. This means that for high power heat/cool applications, high subcooling implications are expected. But on the other hand, for the case of thermal comfort applications, in which PCM is expected to be exposed to slow temperature changes, no important subcooling occurs [27], so general assumptions can be taken.

This subcooling behaviour is induced by the nucleation and growth kinetics of crystals forming the PCM. Consequently, when the sample is cooled rapidly, the crystalline structure grows at a lower temperature, producing this hysteresis effect. Moreover, in the case of PEGs, several types of "crystals" can be formed during the crystallisation and even during storage, which results in different inner structures and different melting/solidification behaviours [27]. They can be observed when multiple melting peaks are found in DSC curves, reflecting a diverse population of crystalline lamellae.

The results of specific heat capacity (c_p) using a continuous determination programme are detailed in Fig. 3. PEG1500 shows a specific heat capacity of 1.59 $J{\cdot}g^{-1}{\cdot}K^{-1}$ and 2.21 $J{\cdot}g^{-1}{\cdot}K^{-1}$ for solid and liquid states at 20 °C and 60 °C, respectively. All thermal properties experimentally evaluated are summarised in Table 2.

3.2. Parametrisation of phase transition models

3.2.1. Static linear model through linear regression

The optimal fitting for the static linear model is described in Eq. (12), which defines the solid-liquid process as a linear function obtained from the experimental data acquired at 5 °C·min^{-1} heating rate.

$$(T) = \begin{cases} 0 & if\ T \leq 38.36 \\ 0.101 \cdot T - 3.856 & if\ 38.36 < T \leq 48.31 \\ 1 & if\ T > 48.31 \end{cases} \quad (12)$$

3.2.2. Static non-linear model through logistic regression

The optimal fitting for the static non-linear model is described in Eq. (13), which defines the solid-liquid process as a non-linear function based on the experimental data obtained at 5 °C·min^{-1} heating rate.

$$\alpha(T) = \frac{1}{\left(1 + \left(\frac{45.848}{T}\right)^{-42.164}\right)^{0.321}} \quad (13)$$

3.2.3. Static hysteresis model

The optimal fitting for the static hysteresis model is described in Eq. (14), which defines the solid-liquid process as two non-linear functions aiming to consider the subcooling behaviour of the material. They were defined using the experimental data obtained at 5 °C·min^{-1} for heating and cooling, respectively.

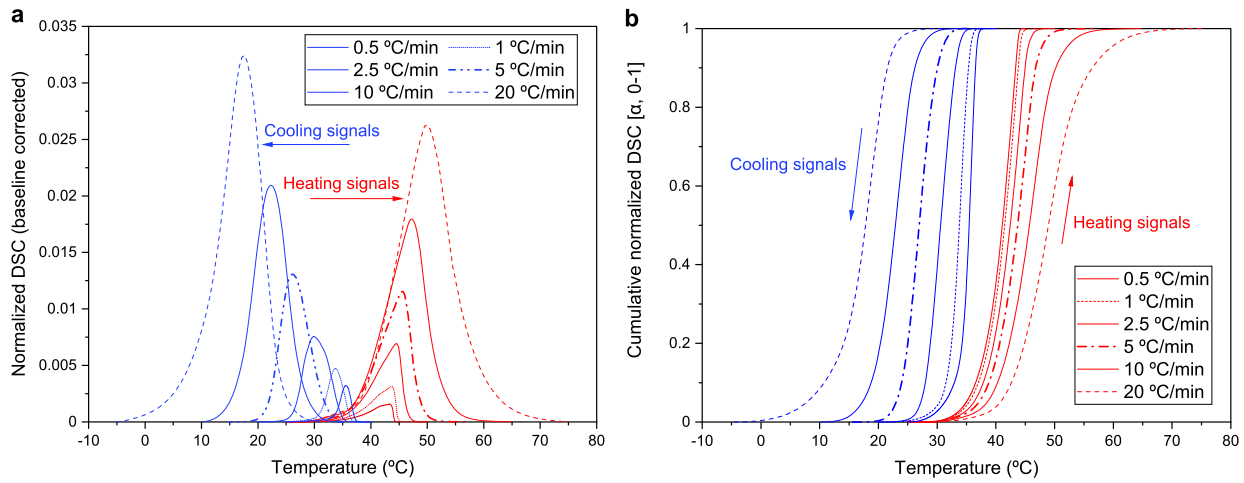

Fig. 2. Normalised DSC signals associated with phase change of PEG1500. a, Normalised DSC signals after baseline correction. b, Cumulative normalised DSC signals representing (liquid mass) phase fractions, from 0 (fully solid) to 1 (fully liquid).

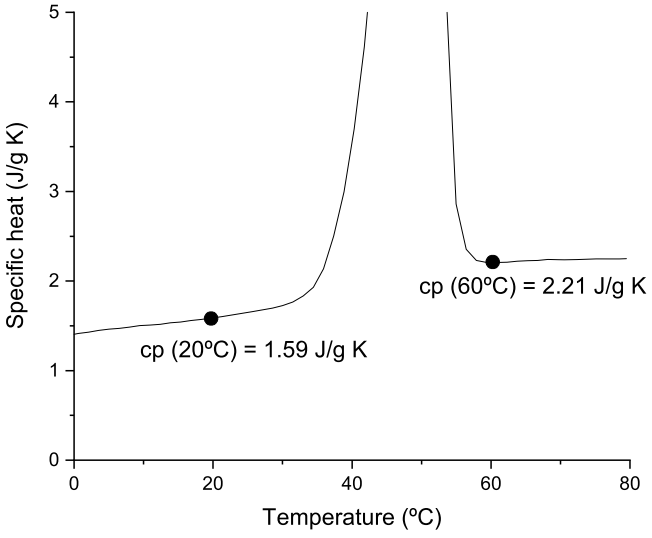

Fig. 3. Specific heat of PEG1500 obtained through a continuous c_p determination programme.

Table 2
Experimental thermal properties of PEG1500.

Property	Units	Values
Melting temperature	°C	37.0
Latent heat	$J{\cdot}g^{-1}$	158.8
Specific heat (solid, 20 °C)	$J{\cdot}g^{-1}{\cdot}K^{-1}$	1.59
Specific heat (liquid, 60 °C)	$J{\cdot}g^{-1}{\cdot}K^{-1}$	2.21

$$\alpha(T) = \frac{1}{\left(1+\left(\frac{45.848}{T}\right)^{-42.164}\right)^{0.321}} \quad if\ sgn\frac{dT}{dt} \geq 0$$
$$\alpha(T) = \frac{1}{\left(1+\left(\frac{27.503}{T}\right)^{-21.537}\right)^{0.747}} \quad if\ sgn\frac{dT}{dt} \leq 0 \qquad (14)$$

3.2.4. Kinetic model

The kinetic model involves the parametrisation of melting phase change as a non-kinetic process and the crystallisation as a kinetic conversion, as was previously demonstrated and justified in Section 3.1. Thus, melting was characterised using the non-linear function defined in Eq. (13), and the kinetic solidification process was parametrised according to the procedure specified in Section 2.3.4, whose results are described as follows.

The apparent activation energy values as a function of the extent of conversion were first determined by a model-free procedure: the Friedman isoconversional analysis. The experimental curves shown in Fig. 2 were analysed simultaneously using Eq. (6). Fig. 4 presents the plots of $ln\left(\frac{d\alpha}{dt}\right)_\alpha$ versus $\frac{1}{T_\alpha}$ for the extent of conversion values in the range 0.2–0.8. The plots can be reasonably well fitted by linear regression. The results show that the activation energy throughout the phase transition is approximately constant, with an average value of -104 ± 3 $kJ{\cdot}mol^{-1}$. These results indicate that the phase transition can be considered a single process that may be described by a unique kinetic triplet.

The experimental data evaluation through the model-fitting (combined kinetic) analysis determined the kinetic triplet (Ea, A and $f(\alpha)$) to simulate the kinetic performance of the material. Fig. 5a includes the plot of $ln\left(\frac{\frac{d\alpha}{dt}}{(1-\alpha)^n\,\alpha^m}\right)$ versus 1/T (Eq. (8)). From the optimisation, the

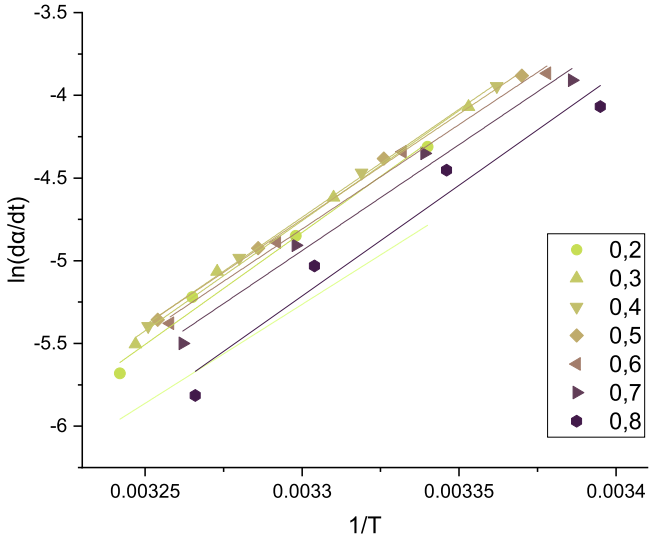

Fig. 4. Friedman plots resulting from the isoconversional analysis for selected α values of the experimental curves presented in Fig. 2.

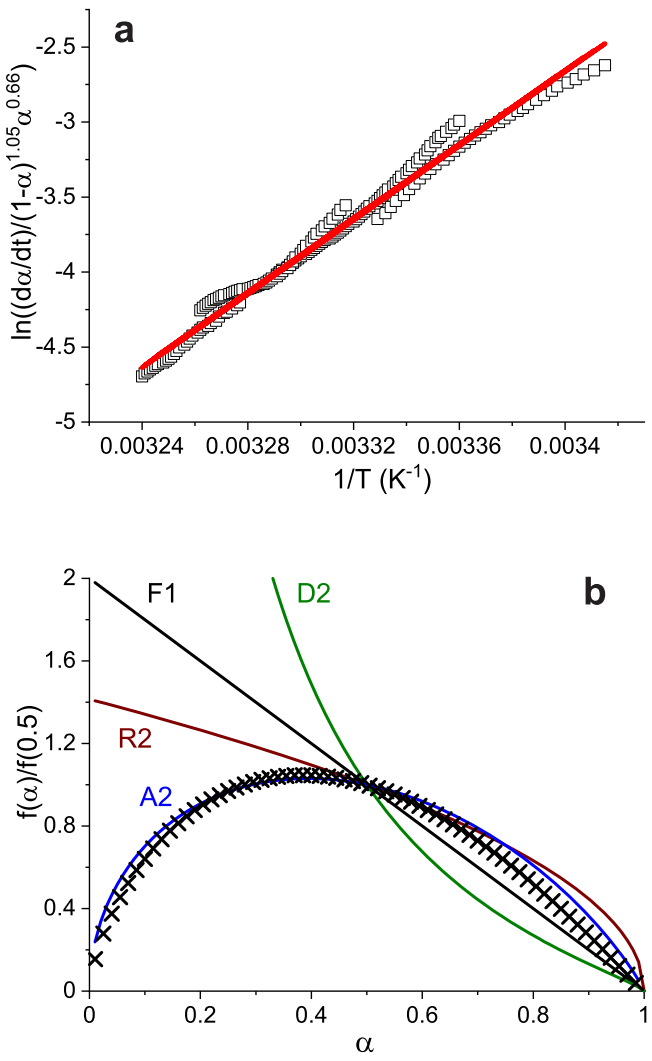

Fig. 5. Plots resulting from the combined kinetic analysis. a, Combined kinetic analysis of experimental curves included in Fig. 2 employing Eq. (8) to determine n and m parameters resulting from the optimisation procedure. b, Comparison of the f(α) functions (solid lines) normalized at α=0.5.

experimental data can be simultaneously fitted into a straight line for n and m values of 1.05 and 0.66, respectively. Interestingly, the slope of the straight lines leads to an apparent activation energy of -110 ± 3 kJ·mol^{-1}, which is in excellent agreement with the result obtained from the Friedman isoconversional analysis. The intercept gives a pre-exponential factor (A) of 1.7·10^{-21} s^{-1}. Therefore, the reaction function obtained from the analysis is $f(\alpha) = (1-\alpha)^{1.05}\ \alpha^{0.66}$. The final results are summarised in Table 3.

The comparison with master plots (Fig. 5b), for the ideal kinetic models reported in the literature (normalised at f(0.5) to better distinguish the different plots), indicates that the experimentally obtained reaction function closely match the ideal model corresponding to A2 nucleation and growth of nuclei (Avrami-Erofeev kinetic model). This kinetic model implies the instantaneous nucleation (saturation of sites capable of nucleation before growth) and the subsequent two-dimensional growth [50]. It is important to remark that the activation energy and the kinetic model have been obtained without previous assumptions regarding the kinetics of the process.

Table 3
Kinetic triplet (Ea, A and $f(\alpha)$) obtained from the combined kinetic analysis.

Parameter	Values
Ea	-110,000 (±3) J·mol^{-1}
A	1.7·10^{-21} s^{-1}
f(α)=(1-α)^{n}α^m	n=1.053; m=0.66
R	8.3145 J·K^{-1}·mol^{-1}

3.3. Evaluation of phase transition models through temperature induced

The results obtained for the parametrisation of phase transition models, defined in Section 3.2, are evaluated and compared in this section through complete and incomplete phase transitions. In this evaluation, the temperature is considered as an input value to the different phase transition models. The simulated results of conversion progress (α), from 0 (fully solid state) to 1 (fully liquid state), are plotted in relation to experimental results obtained at 5 °C·min^{-1} as reference values: melting curve plotted as a dashed red line and crystallisation curve as a dashed blue line.

Fig. 6. shows the simulated results of phase transition models with temperature induced through a heating/cooling rate decreasing throughout the time with the following velocities: 10, 5, 2.5, 1 and 0.5 °C·min^{-1}.

The results reproduce the "complete phase transition progress" obtained through these temperature profiles, showing a large deviation between the proposed phase change modelling approaches. These discrepancies between measured and simulated data are mainly due to the subcooling effect and the kinetic-dependent behaviour of the material.

For the case of kinetic-independent phase transition models, the static linear model (Fig. 6a), characterised by a linear function, represents the simplest phase transition model; and the static non-linear model (Fig. 6b) involves the non-linear progression of phase transition, smoothing the change in the slop. Both curves fit well at a heating rate of 5 °C·min^{-1}. However, they lack the consideration of PCM subcooling, which has an important impact on crystallisation temperature. Static hysteresis (Fig. 6c) solves this issue, including an additional curve and fitting PCM's global phase transition behaviour during melting and crystallisation. However, all these models only depend on temperature but not on the heating/cooling rate. Thus, a faster or slower heating/cooling rate will not change the shape of the T-α graphs.

The kinetic model (Fig. 6d), or kinetic-dependent model, solves this issue by considering the heating/cooling rate during the phase transition. The simulated results in Fig. 6d show how the material's melting follows a kinetic-independent evolution, as was previously demonstrated by the experimental results. Conversely, crystallisation is highly affected by the kinetics of the process. In this process, the subcooling delay decreases with the reduction of the cooling rate, resulting in significantly reduced subcooling at low cooling rates.

This kinetic model can be explained in terms of instantaneous nucleation (saturation of sites capable of nucleation prior to growth) and a phase boundary controlled two-dimensional growth of the nuclei, either in bulk or on the surface. Alternatively, it could be interpreted as a constant rate of homogeneous nucleation during the process followed by a bulk phase-boundary controlled one-dimensional growth or diffusion-controlled two-dimensional growth, either in bulk on or the surface [50].

The results confirm the potential of the kinetic approach for a more reliable thermal performance modelling of PCM, above all during energy balance applications that can involve different heating/cooling rates during heat transfer. Moreover, it is highlighted the significant deviation of PCM transitions obtained at large heating/cooling rates, which can introduce large errors when studying low rate heat transfer applications. Considering that typical heating/cooling rates for material characterisation are 5 °C·min^{-1}, 10 °C·min^{-1} and even 20 °C·min^{-1}, special attention should be focused on more appropriate material parametrisation through kinetic modelling.

Fig. 7 shows the simulated results of phase transition models with a temperature test profile alternating during incomplete melting and

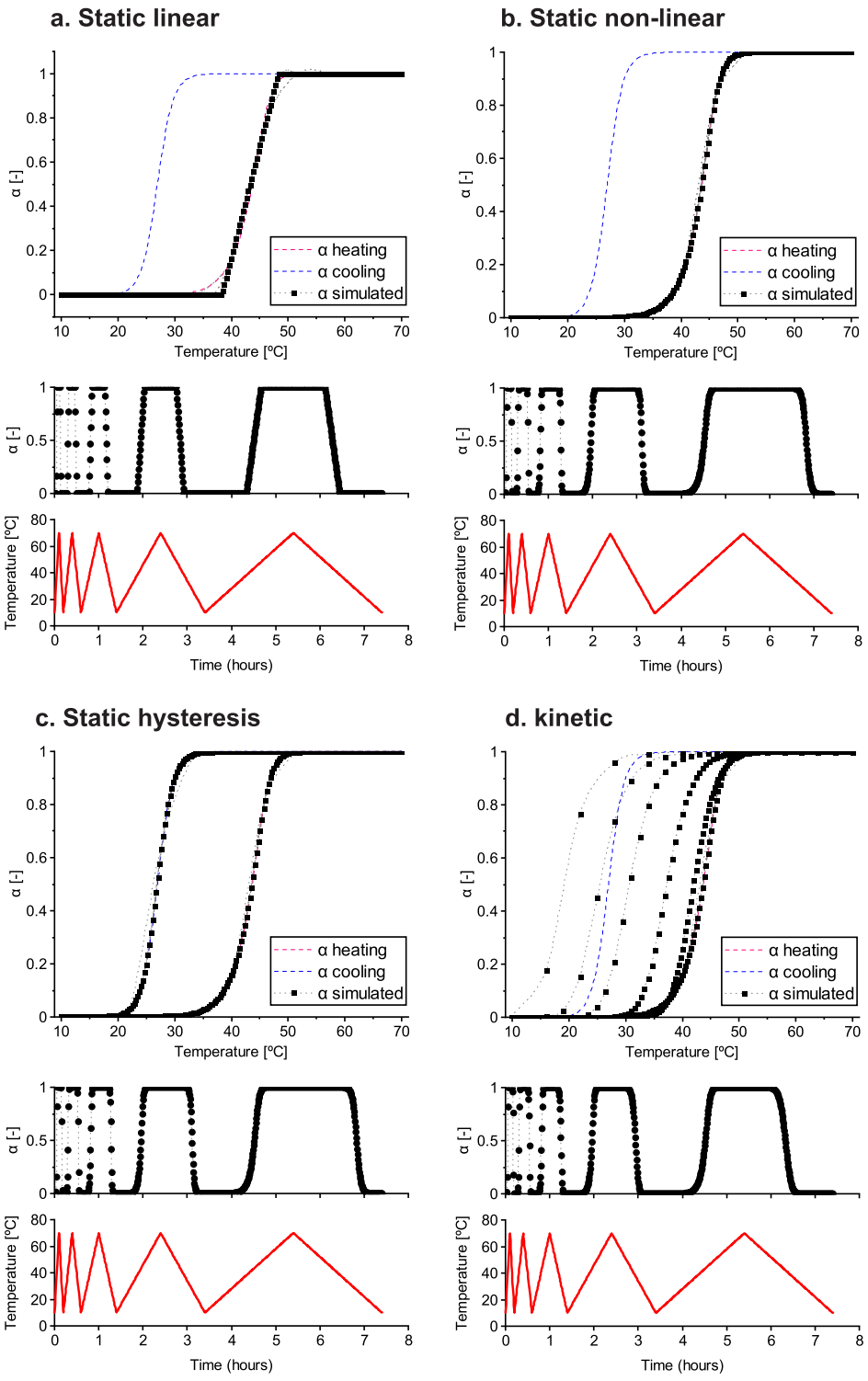

Fig. 6. Simulations of phase transition models with temperature induced through a heating/cooling rate decreasing with time (10, 5, 2.5, 1 and 0.5 °C·min^{-1}). Simulation time step of 0.01 hour. First plot: predicted phase fractions (α) as a function of temperature. Second: predicted phase fractions (α) as a function of time. Third: temperature profile induced as a function of time.

solidification states. Thus, the selected maximum and minimum temperatures between heating/cooling ramps are located inside the temperature range of PCM's melting/solidification phase. Moreover, the rate is increased with time (1, 2.5 and 5 °C·min^{-1}).

These results reproduce the PCM evolution during "incomplete phase transition progress", showing even large deviations between the proposed modelling alternatives.

For the case of kinetic-independent phase transition models, the static linear model (Fig. 7a) and static non-linear model (Fig. 7b) produce a complete solidification in all cooling cycles. The only difference arises in the large number of dots obtained using the non-linear function at the end of phase change, but it barely modifies the conversion situation. On the other hand, the static hysteresis approach (Fig. 7c) shows completely different behaviour. In this phase change modelling

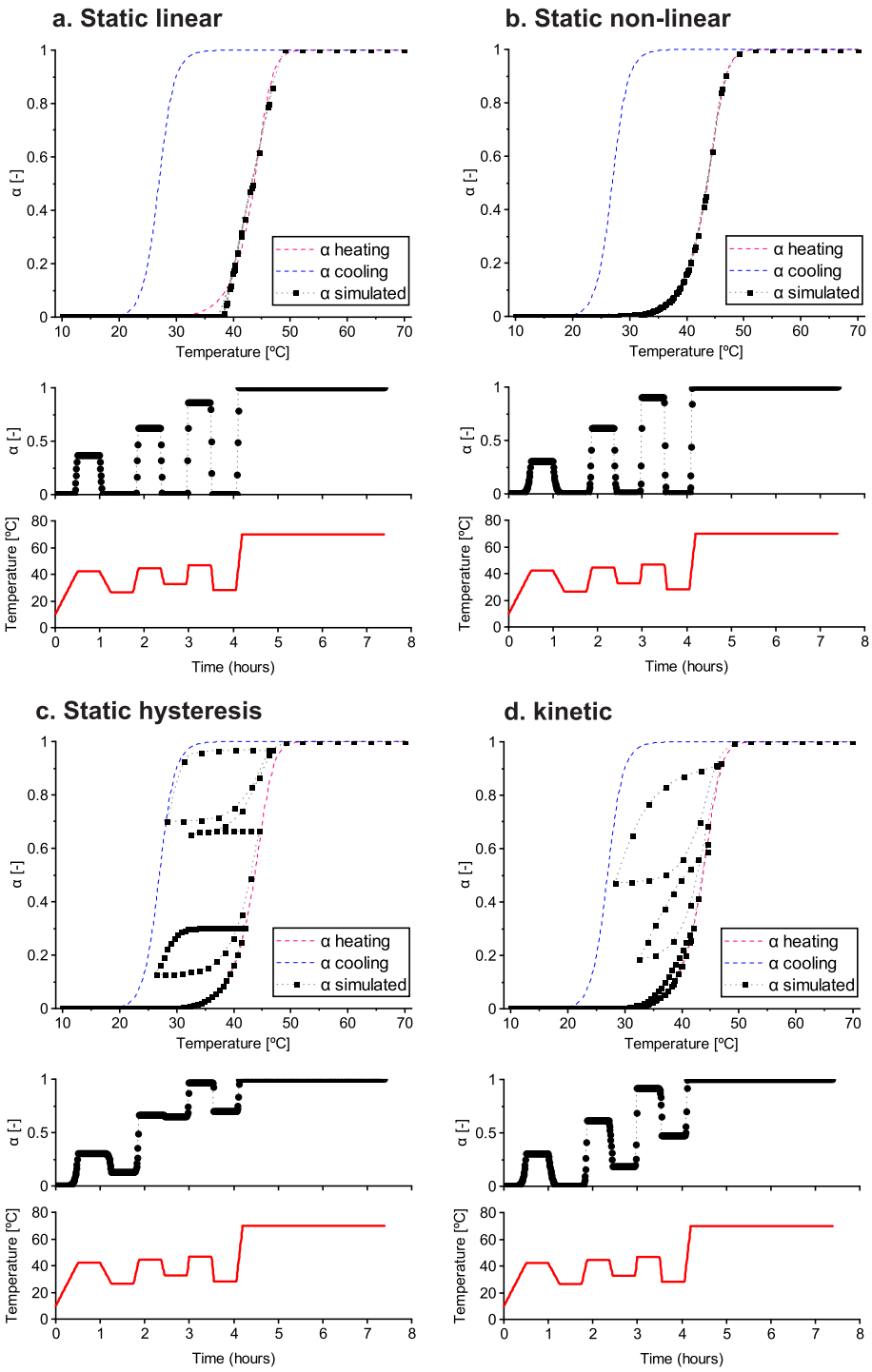

Fig. 7. Simulations of phase transition models for a temperature profile where heating and cooling ramps are reversed during incomplete phase change and heating/cooling rate increases with time (1, 2.5 and 5 °C·min^{-1}). Simulation time step of 0.01 hour. First plot: predicted phase fractions (α) as a function of temperature. Second: predicted phase fractions (α) as a function of time. Third: temperature profile induced as a function of time.

approach, when the temperature rate is reversed in an incomplete phase change state, the degree of conversion remains constant until another hysteresis is reached. This means that during the cooling period introduced at the incomplete melting process, the phase change remains constant without the solidification of the material. This is an unrealistic and different PCM behaviour compared to the static linear model (Fig. 7a) or static non-linear model (Fig. 7b), where a complete solidification state is achieved. Moreover, a faster or slower heating/cooling rate during incomplete phase change will not change the shape of the T-α graphs.

An intermediate and more realistic phase change behaviour is found through the kinetic model (Fig. 7d), in which the degree of conversion is situated at a middle point with regard to previously discussed kinetic-independent phase transition models. In this case, the phase change does not remain constant during the reverse cycle, but it also does not develop fully. The phase change is always in evolution following a kinetic-dependent transition. The results show that the higher the cooling rate, the more significant the subcooling hysteresis. These

results demonstrate the reliable phase conversion during complete and incomplete cycles using a kinetic model compared to kinetic-independent phase transition models. The following section evaluates the accuracy of each modelling approach and will determine criteria and guidelines for their use in energy balance problems.

3.4. Statistical comparison of phase transition models for heat transfer in energy balance models

In the case of heat transfer using PCM in energy balance models, the temperature will be the output value (simulated value), as a result of energy balance equations. In this situation, an appropriate characterisation of thermal properties should be defined through an apparent heat capacity curve or an enthalpy-temperature function, involving a kinetic-dependent or a kinetic-independent phase transition model. Aiming to compare the benefits of the kinetic approach in comparison with conventional modelling approaches, the apparent heat capacity situation for different heat transfer rates is evaluated per each modelling alternative in order to calculate their accuracy and determine criteria and guidelines for optimal thermal parametrisation of PCM.

Fig. 8 illustrates the comparison of apparent heat capacity simulated through different phase transition models at different rates. Fig. 8a shows the melting and solidification curves at a rate of 1 °C·min^{-1}, Fig. 8b at 5 °C·min^{-1} and Fig. 8c at 10 °C·min^{-1}. The simulated results are compared with apparent heat capacity (dashed black line) obtained through experimental data previously shown in Section 3.1.

The apparent heat capacity curves simulated during heating (melting process) are kinetic-independent processes with no modification of partial enthalpy distribution per phase transition model and rate. The simulated curves are based on experimental results obtained at 5 °C·min^{-1} for melting, illustrated in Fig. 8b (dashed black line), where the simulated curves better fit the experimental ones. The slight difference between simulated and measured curves at lower and higher rates (Fig. 8a and 8c) are mainly related to heat conduction in the pans, heat transfer and apparatus design [17].

A different situation occurs when apparent heat capacity curves are simulated during cooling, following a kinetic-dependent phase transition. In this case, the kinetic-independent and kinetic-dependent models show completely different results when compared with experimental curves. The conventional models (static linear model, static non-linear model and static hysteresis model) have the best fitting at a rate of 5 °C·min^{-1} (Fig. 8b). This is mainly because the simulated partial enthalpy

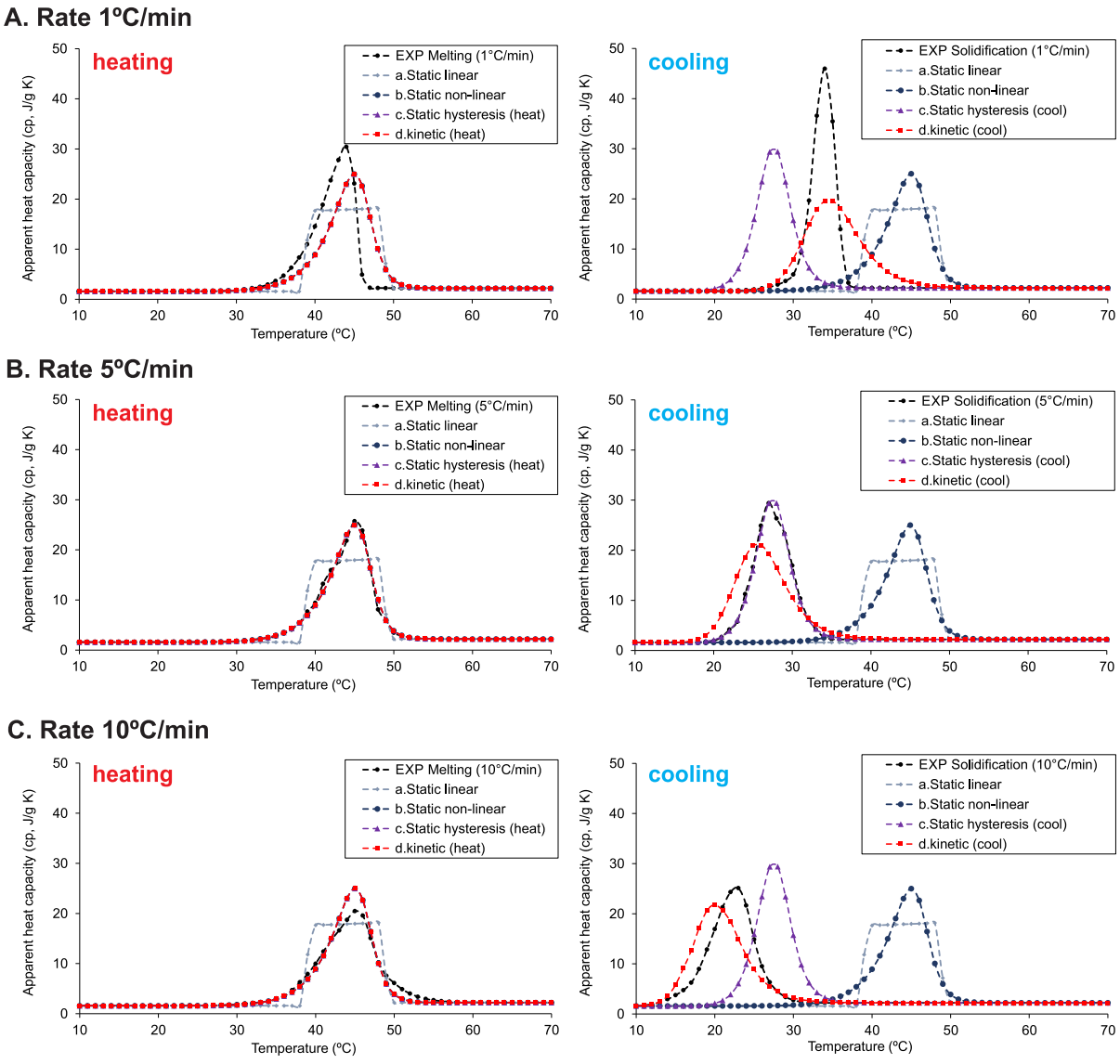

Fig. 8. Comparison of apparent heat capacity obtained through different phase transition models at different rates.

distribution during crystallisation was parametrised using experimental data obtained at 5 °C·min^{-1}. However, a large deviation is found when lower and higher rates are compared (Fig. 8a and c), resulting in a significant error in the apparent heat capacity calculation for all kinetic-independent models. This accuracy problem is solved by using the kinetic approach, which provides a kinetic-dependent phase transition. The kinetic model completely adapts the partial enthalpy distribution per cooling rate, obtaining better matching between measured and simulated values at 1 °C/min and 10 °C/min.

These simulated results are statistically compared with measured experimental curves through the coefficient of determination (R^2) in Table 4. This is a statistical index commonly used to measure the uncertainty of the models. The results are between 0.00 and 1.00, where the upper value means that the simulated values match the measured ones perfectly.

Static linear and static non-linear models do not show high differences between them, but they provide the worst fitting during cooling transitions by not considering the effect of subcooling (hysteresis). The lack of hysteresis consideration results in lower accuracy, obtaining an R^2 of 0.40 and 0.45, respectively. Static hysteresis overcomes this issue, but only when the simulated cooling rate matches the measured process rate at 5 °C·min^{-1}, which improves the R^2 statistical index at 0.61. Finally, the results show how the kinetic approach provides higher accuracy between measured and simulated values, obtaining an R^2 of 0.80. These results demonstrate the benefits of kinetic models for heat transfer applications involving phase change materials.

This paper introduces for the first time a complete parametrisation and experimental validation of the kinetic model using PEG1500 as a reference material, whose results demonstrate the higher accuracy and benefits of the kinetic modelling for phase change transitions. However, further studies are required to thoroughly validate the extended use of the kinetic approach for PCM modelling.

4. Conclusions

This paper proposes an advanced parametrisation of phase change materials (PCM) through a kinetic approach and compares it with three typical parametrisation alternatives based on static linear, static non-linear and static hysteresis models. A complete kinetic evaluation and parametrisation of PEG1500 were developed by both model-free (iso-conversional) and combined kinetic procedures. Based on the results, it is possible to extract the following conclusions:

A strong influence of kinetics was found in the crystallisation phase transition of PEG1500, showing different subcooling grades in their hysteresis under different temperature rates.

The comparison of parametrised phase transition models clearly indicates the potential of the kinetic approach for a more reliable thermal parametrisation of PCM, above all during energy balance applications that can involve different heating/cooling rates during heat transfer. The statistical comparison between models demonstrates the higher accuracy of the kinetic approach to correctly represent the partial enthalpy distribution of PCMs, obtaining a coefficient of determination (R^2) of 0.80. On the other hand, the accuracy of conventional (or kinetic-independent) models is limited between 0.40 and 0.61, mainly due to the poor matching when different cooling rates are involved in phase change processes.

The results highlight the importance of kinetics in the phase transition processes, which should be considered in numerical studies for a more reliable and accurate evaluation.

CRediT authorship contribution statement

Jesus Lizana: Conceptualization, Data curation, Formal analysis, Investigation, Methodology, Software, Visualization, Writing – original draft. **Antonio Perejón:** Formal analysis, Methodology, Software, Visualization, Writing – original draft. **Pedro E. Sanchez-Jimenez:** Data curation, Funding acquisition, Methodology, Resources, Supervision, Writing – review & editing. **Luis A. Perez-Maqueda:** Conceptualization, Formal analysis, Funding acquisition, Investigation, Methodology, Project administration, Writing – review & editing.

Table 4
Statistical comparison of apparent heat capacity curves obtained through simulated models and experimental data.

Phase change modelling approaches and rates	R2 (heating)	R2 (cooling)	Mean R2
a. Static linear			
Rate 1 °C/min	0.59	0.02	0.40
Rate 5 °C/min	0.83	0.04	
Rate 10 °C/min	0.88	0.05	
b. Static non-linear			
Rate 1 °C/min	0.65	0.01	0.45
Rate 5 °C/min	0.99	0.03	
Rate 10 °C/min	0.98	0.05	
c. Static hysteresis			
Rate 1 °C/min	0.65	0.00	0.61
Rate 5 °C/min	0.99	0.99	
Rate 10 °C/min	0.98	0.04	
d. kinetic			
Rate 1 °C/min	0.65	0.64	0.80
Rate 5 °C/min	0.99	0.77	
Rate 10 °C/min	0.98	0.75	

Declaration of Competing Interest

The authors declare that they have no known competing financial interests or personal relationships that could have appeared to influence the work reported in this paper.

Acknowledgements

The authors gratefully acknowledge the Spanish Ministry of Science and Innovation's financial support via a Juan de la Cierva Postdoctoral Fellowship granted to Jesús Lizana (FJC2019-039480-I). Financial support from Project CTQ2017-83602-C2-1-R (MINECO-FEDER) and Project 201960E092 (INTRAMURAL-CSIC) is acknowledged. This research was also supported by the European Union's Horizon 2020 research and innovation programme under the Marie Skłodowska-Curie grant agreement No 101023241. We also acknowledge the funding received by Junta de Andalucía-Consejería de Economía, Conocimiento, Empresas y Universidad and FEDER (projects P18-FR-1087 and US-1262507).

References

[1] J. Lizana, R. Chacartegui, A. Barrios-Padura, C. Ortiz, Advanced low-carbon energy measures based on thermal energy storage in buildings: a review, Renewable Sustainable Energy Rev. 82 (2018) 3705–3749, https://doi.org/10.1016/j.rser.2017.10.093.

[2] Z. Yin, J. Zheng, H. Kim, Y. Seo, P. Linga, Hydrates for cold energy storage and transport: a review, Adv. Appl. Energy 2 (2021), 100022, https://doi.org/10.1016/j.adapen.2021.100022.

[3] P.B. Salunkhe, D. Jaya Krishna, Investigations on latent heat storage materials for solar water and space heating applications, J. Energy Storage 12 (2017) 243–260, https://doi.org/10.1016/j.est.2017.05.008.

[4] J. Lizana, C. Bordin, T. Rajabloo, Integration of solar latent heat storage towards optimal small-scale combined heat and power generation by Organic Rankine Cycle, J. Energy Storage 29 (2020), 101367, https://doi.org/10.1016/j.est.2020.101367.

[5] H. Mousa, J. Naser, O. Houche, Using PCM as energy storage material in water tanks: theoretical and experimental investigation, J. Energy Storage 22 (2019) 1–7, https://doi.org/10.1016/j.est.2019.01.018.

[6] J. Lizana, R. Chacartegui, A. Barrios-Padura, J.M. Valverde, C. Ortiz, Identification of best available thermal energy storage compounds for low-to-moderate temperature storage applications in buildings, Materiales de Construcción 68 (2018) 1–35, https://doi.org/10.3989/mc.2018.10517.

[7] J. Lizana, R. Chacartegui, A. Barrios-Padura, J.M. Valverde, Advances in thermal energy storage materials and their applications towards zero energy buildings: a

critical review, Appl. Energy 203 (2017) 219–239, https://doi.org/10.1016/j.apenergy.2017.06.008.
[8] H. Asgharian, E. Baniasadi, A review on modeling and simulation of solar energy storage systems based on phase change materials, J. Energy Storage 21 (2019) 186–201, https://doi.org/10.1016/j.est.2018.11.025.
[9] L.F. Cabeza, Advances in Thermal Energy Storage Systems. Methods and Applications, Woodhead Publishing, 2014.
[10] P. Tan, P. Lindberg, K. Eichler, P. Löveryd, P. Johansson, A.S. Kalagasidis, Thermal energy storage using phase change materials: techno-economic evaluation of a cold storage installation in an office building, Appl. Energy 276 (2020), 115433, https://doi.org/10.1016/j.apenergy.2020.115433.
[11] T. Barz, J. Krämer, J. Emhofer, Identification of phase fraction-temperature curves from heat capacity data for numerical modeling of heat transfer in commercial paraffin waxes, Energies (2020) 13, https://doi.org/10.3390/en13195149.
[12] F. Ascione, N. Bianco, R.F. De Masi, F. de' Rossi, G.P. Vanoli, Energy refurbishment of existing buildings through the use of phase change materials: energy savings and indoor comfort in the cooling season, Appl. Energy 113 (2014) 990–1007, https://doi.org/10.1016/j.apenergy.2013.08.045.
[13] B.M. Diaconu, M. Cruceru, Novel concept of composite phase change material wall system for year-round thermal energy savings, Energy Build. 42 (2010) 1759–1772, https://doi.org/10.1016/j.enbuild.2010.05.012.
[14] J. Lizana, D. Friedrich, R. Renaldi, R. Chacartegui, Energy flexible building through smart demand-side management and latent heat storage, Appl. Energy 230 (2018) 471–485, https://doi.org/10.1016/j.apenergy.2018.08.065.
[15] H. Xu, Y. Wang, X. Han, Analytical considerations of thermal storage and interface evolution of a PCM with/without porous media, Int. J. Numer. Methods Heat Fluid Flow 30 (2020) 373–400, https://doi.org/10.1108/HFF-02-2019-0094.
[16] H.J. Xu, C.Y. Zhao, Thermal efficiency analysis of the cascaded latent heat/cold storage with multi-stage heat engine model, Renewable Energy 86 (2016) 228–237, https://doi.org/10.1016/j.renene.2015.08.007.
[17] T. Barz, A. Sommer, Modeling hysteresis in the phase transition of industrial-grade solid/liquid PCM for thermal energy storages, Int. J. Heat Mass Transfer 127 (2018) 701–713, https://doi.org/10.1016/j.ijheatmasstransfer.2018.08.032.
[18] T. Barz, J. Emhofer, K. Marx, G. Zsembinszki, L.F. Cabeza, Phenomenological modelling of phase transitions with hysteresis in solid/liquid PCM, J. Building Perform. Simul. 12 (2019) 770–788, https://doi.org/10.1080/19401493.2019.1657953.
[19] M. Zukowski, Mathematical modeling and numerical simulation of a short term thermal energy storage system using phase change material for heating applications, Energy Convers. Manage. 48 (2007) 155–165, https://doi.org/10.1016/j.enconman.2006.04.017.
[20] C. Piselli, M. Prabhakar, A. de Gracia, M. Saffari, A.L. Pisello, L.F. Cabeza, Optimal control of natural ventilation as passive cooling strategy for improving the energy performance of building envelope with PCM integration, Renewable Energy 162 (2020) 171–181, https://doi.org/10.1016/j.renene.2020.07.043.
[21] K. Biswas, J. Lu, P. Soroushian, S. Shrestha, Combined experimental and numerical evaluation of a prototype nano-PCM enhanced wallboard, Appl. Energy 131 (2014) 517–529, https://doi.org/10.1016/j.apenergy.2014.02.047.
[22] Y. Hu, P.K. Heiselberg, A new ventilated window with PCM heat exchanger—performance analysis and design optimization, Energy Build. 169 (2018) 185–194, https://doi.org/10.1016/j.enbuild.2018.03.060.
[23] E. Moreles, G. Huelsz, G. Barrios, Hysteresis effects on the thermal performance of building envelope PCM-walls, Building Simul. 11 (2018) 519–531, https://doi.org/10.1007/s12273-017-0426-4.
[24] J. Lizana, M. De-Borja-Torrejon, A. Barrios-Padura, T. Auer, R. Chacartegui, Passive cooling through phase change materials in buildings. A critical study of implementation alternatives, Appl. Energy 254 (2019) 1–17, https://doi.org/10.1016/j.apenergy.2019.113658.
[25] A. Caggiano, C. Mankel, E. Koenders, Reviewing theoretical and numerical models for PCM-embedded cementitious composites, Buildings (2018) 9, https://doi.org/10.3390/buildings9010003.
[26] L. Klimes, P. Charvat, M. Ostry, Challenges in the computer modeling of phase change materials, Mater. Technol. 46 (2012) 335–338.
[27] R. Paberit, E. Rilby, J. Göhl, J. Swenson, Z. Refaa, P. Johansson, H. Jansson, Cycling stability of poly(ethylene glycol) of six molecular weights: influence of thermal conditions for energy applications, ACS Appl. Energy Mater. 3 (2020) 10578–10589, https://doi.org/10.1021/acsaem.0c01621.
[28] L.A. Pérez-Maqueda, J.M. Criado, P.E. Sánchez-Jiménez, Combined kinetic analysis of solid-state reactions: a powerful tool for the simultaneous determination of kinetic parameters and the kinetic model without previous assumptions on the reaction mechanism, J. Phys. Chem. A 110 (2006) 12456–12462, https://doi.org/10.1021/jp064792g.
[29] S. Vyazovkin, A.K. Burnham, J.M. Criado, L.A. Pérez-Maqueda, C. Popescu, N. Sbirrazzuoli, ICTAC kinetics committee recommendations for performing kinetic computations on thermal analysis data, Thermochim. Acta 520 (2011) 1–19, https://doi.org/10.1016/j.tca.2011.03.034.
[30] F.J. Gotor, M.Criado José, J. Malek, N. Koga, Kinetic analysis of solid-state reactions: the universality of master plots for analyzing isothermal and nonisothermal experiments, J. Phys. Chem. A 104 (2000) 10777–10782, https://doi.org/10.1021/jp0022205.
[31] S. Vyazovkin, N. Koga, C. Schick, Handbook of Thermal Analysis and Calorimetry. Volume 6. Recent Advances, Techniques and Applications, 2nd ed., Elsevier, 2018.
[32] L.A. Pérez-Maqueda, A. Ortega, J.M. Criado, The use of master plots for discriminating the kinetic model of solid state reactions from a single constant-rate thermal analysis (CRTA) experiment, Thermochim. Acta 277 (1996) 165–173, https://doi.org/10.1016/0040-6031(95)02746-7.
[33] L.A. Pérez-Maqueda, P.E. Sánchez-Jiménez, J.M. Criado, Evaluation of the integral methods for the kinetic study of thermally stimulated processes in polymer science, Polymer 46 (2005) 2950–2954, https://doi.org/10.1016/j.polymer.2005.02.061.
[34] S. Vyazovkin, Isoconversional Kinetics of Thermally Stimulated Processes, Springer, 2015, https://doi.org/10.1007/978-3-319-14175-6.
[35] E.I. Mohamed Moussa, M. Karkri, A numerical investigation of the effects of metal foam characteristics and heating/cooling conditions on the phase change kinetic of phase change materials embedded in metal foam, J. Energy Storage 26 (2019), 100985, https://doi.org/10.1016/j.est.2019.100985.
[36] Y. Wu, X. Zhang, X. Xu, X. Lin, L. Liu, A review on the effect of external fields on solidification, melting and heat transfer enhancement of phase change materials, J. Energy Storage 31 (2020), 101567, https://doi.org/10.1016/j.est.2020.101567.
[37] F. Agyenim, N. Hewitt, P. Eames, M. Smyth, A review of materials, heat transfer and phase change problem formulation for Latent Heat Thermal Energy Storage Systems (LHTESS), Renewable Sustainable Energy Rev. 14 (2010) 615–628.
[38] S. Vyazovkin, K. Chrissafis, M.L. Di Lorenzo, N. Koga, M. Pijolat, B. Roduit, N. Sbirrazzuoli, J.J. Suñol, ICTAC kinetics committee recommendations for collecting experimental thermal analysis data for kinetic computations, Thermochim. Acta 590 (2014) 1–23, https://doi.org/10.1016/j.tca.2014.05.036.
[39] Y. Kou, S. Wang, J. Luo, K. Sun, J. Zhang, Z. Tan, Q. Shi, Thermal analysis and heat capacity study of polyethylene glycol (PEG) phase change materials for thermal energy storage applications, J. Chem. Thermodyn. 128 (2019) 259–274, https://doi.org/10.1016/j.jct.2018.08.031.
[40] H.L. Friedman, Kinetics of thermal degradation of char-forming plastics from thermogravimetry. Application to a phenolic plastic, J. Polym. Sci. Part C 6 (1964) 183–195, https://doi.org/10.1002/polc.5070060121.
[41] J.M. Criado, P.E. Sánchez-Jiménez, L.A. Pérez-Maqueda, Critical study of the isoconversional methods of kinetic analysis, J. Therm. Anal. Calorim. 92 (2008) 199–203, https://doi.org/10.1007/s10973-007-8763-7.
[42] P.E. Sánchez-Jiménez, L.A. Pérez-Maqueda, A. Perejón, J.M. Criado, Combined kinetic analysis of thermal degradation of polymeric materials under any thermal pathway, Polym. Degrad. Stab. 94 (2009) 2079–2085, https://doi.org/10.1016/j.polymdegradstab.2009.07.006.
[43] Y. Ivshin, T.J. Pence, A constitutive model for hysteretic transition behavior, Int. J. Eng. Sci. 32 (1994) 681–704, https://doi.org/10.1016/0020-7225(94)90027-2.
[44] U. Gaur, B. Wunderlic, Heat capacity and other thermodynamic properties of linear macromolecules. II. Polyethylene, J. Phys. Chem. Ref. Data 10 (1981) 119–152, https://doi.org/10.1063/1.555678.
[45] H. Hu, S.A. Argyropoulos, Mathematical modelling of solidification and melting: a review, Model. Simul. Mater. Sci. Eng. 4 (1996) 371–396, https://doi.org/10.1088/0965-0393/4/4/004.
[46] D. Chicco, M.J. Warrens, G. Jurman, The coefficient of determination R-squared is more informative than SMAPE, MAE, MAPE, MSE and RMSE in regression analysis evaluation, PeerJ Comput. Sci. 7 (2021) 1–24, https://doi.org/10.7717/PEERJ-CS.623.
[47] J.L. Devore, Probability and Statistics for Engineering and the Sciences, 8th ed., MA: Cengage Learning, Boston, 2011.
[48] Z. Refaa, M. Boutaous, S. Xin, D.A. Siginer, Thermophysical analysis and modeling of the crystallization and melting behavior of PLA with talc: kinetics and crystalline structures, J. Therm. Anal. Calorim. 128 (2017) 687–698, https://doi.org/10.1007/s10973-016-5961-1.
[49] J. Göhl, R. Paberit, E. Rilby, J. Swenson, P. Johansson, H. Jansson, Manipulation of phase transition temperatures and supercooling of sugar alcohols based Phase Change Materials (PCMs) by urea, in: INNOSTORAGE Conference, 2016, pp. 16–19.
[50] L.A. Pérez-Maqueda, J.M. Criado, J. Málek, Combined kinetic analysis for crystallization kinetics of non-crystalline solids, J. Non Cryst. Solids 320 (2003) 84–91, https://doi.org/10.1016/S0022-3093(03)00023-1.